Controlled Plasmon Resonance of Gold Nanoparticles Self-Assembled with PAMAM Dendrimers

Sudhanshu Srivastava, Benjamin L. Frankamp, and Vincent M. Rotello*

Department of Chemistry, University of Massachusetts, Amherst 01003

Received August 24, 2004. Revised Manuscript Received October 30, 2004

Self-assembly of optically active gold nanoparticles with varying generations of poly(amidoamine) (PAMAM) dendrimers provides aggregates with controlled interparticle spacing, as determined using small-angle X-ray scattering (SAXS). This structural control provides a method for systematically shifting the surface plasmon resonance (SPR) of the particles, based on the decrease in dipolar coupling with increased interparticle distance. Through choice of dendrimer generation, we were able to tune interparticle spacing over a 2.1 nm range, resulting in an 84 nm shift in the SPR. This modulation demonstrates the feasibility of using dendrimer assembly to tune the optical properties of materials.

The plasmonics of noble metal nanoparticle materials is the subject of intense research[1] and has found a many uses, ranging from sensors[2] to optical materials.[3] In general, the surface plasmon resonance (SPR)[4] of metallic nanoparticles are controlled by a complex mixture of factors, including the refractive index of the ligand coating and the surrounding solvent, the core size, and the dipolar coupling.[5,6] It has been shown that SPR can be controlled by particle−particle interaction dictated by interparticle distance[7,8] and the particle volume.[9,10] Recently, Mulvaney and co-workers investigated the dependence of SPR on interparticle spacing through controlled growth of a silica layer on gold cores.[11] They found that the SPR was strongly dependent on the interparticle distance and could be fit to the Maxwell−Garnett effective medium theory.[12] Their foundational work prompted us to seek more efficient and versatile ways to control interparticle spacing of optically active nanoparticles.

Controlled nanoparticle self-assembly resulting in functional materials holds great promise for many practical applications.[13] A significant obstacle to this reality is the lack of tunable self-assembly methods that are designed to accommodate a wide variety of functional nanoparticles. We recently reported on one such method involving dendrimer-mediated assembly of 2 nm gold nanoparticles resulting in well-controlled aggregates.[14] Through choice of dendrimer generation we were able to systematically control the interparticle spacing in the resulting dendrimer/nanoparticle composite. Due to our choice of particle, however, this structural variation did not result in a functional response. However, the method we employed is designed to be versatile, allowing us to insert a particle that features inherent functionality and control of the collective behavior of the assembly based on dendrimer generation (Figure 1).

In this study we describe the synthesis and self-assembly of gold nanoparticles with inherent optical properties. Starting with thiol-passivated gold particles, we used thermal ripening[15] and the Murray place exchange reaction to create a nanoparticle featuring highly monodisperse cores and a carboxylic acid functionalized monolayer (MMPC **1**).[16] Poly(amidoamine) PAMAM dendrimers[17] of generations 0, 1, 2, and 4, (G_0, G_1, G_2, G_4) were used to assemble and systematically control the interparticle spacing between

* Corresponding author: E-mail: rotello@chem.umass.edu.

(1) Wessels, J. M.; Nothofer, H. G.; Ford, W. E.; von Wrochem, F.; Scholz, F.; Vossmeyer, T.; Schroedter, A.; Weller, H.; Yasuda, A. *J. Am. Chem. Soc.* **2004**, *126*, 3349−3356.
(2) Sun, Y. G.; Xia, Y. N. *Anal. Chem.* **2002**, *74*, 5297−5305.
(3) (a) Sershen, S. R.; Westcott, S. L.; West, J. L.; Halas, N. J. *Appl. Phys. B−Lasers Opt.* **2001**, *73*, 379. (b) Tominaga, J. *J. Phys.-Condes. Matter* **2003**, *15*, R1101−R1122.
(4) (a) Kreilbig, U.; Vollmer, M. *Optical Properties of Metal Clusters*; Springer-Verlag: Berlin, 1996. (b) Wei, A. *Nanoparticles Building blocks for Nanotechnology*; Rotello, V. M.; Kluwer Academic/Plenium Publishers: New York, 2004; pp 173−200.
(5) (a) Homola, J. *Anal. Bioanal. Chem.* **2003**, *377*, 528−539, (b) Saponjic, Z. V.; Csencsits, R.; Rajh, T.; Dimitrijevic, N. M. *Chem. Mater.* **2003**, *15*, 4521−4526.
(6) McConnell, W. P.; Novak, J. P.; Brousseau, L. C.; Fuierer, R. R.; Tenent, R. C.; Feldheim, D. L. *J. Phys. Chem. B* **2000**, *104*, 8925−8930.
(7) Rechberger, W.; Hohenau, A.; Leitner, A.; Krenn, J. R.; Lamprecht, B.; Aussenegg, F. R. *Opt. Commun.* **2003**, *220*, 137−141.
(8) (a) Schmitt, J.; Decher, G.; Dressick, W. J.; Brandow, S. L.; Geer, R. E.; Shashidhaar, R.; Calvert, J. M. *Adv. Mater.* **1997**, *9*, 61−65. (b) Malikova, N.; Pastoriza-Santos, I.; Schierhorn, M.; Kotov, N. A.; Liz-Marzan, L. M. *Langmuir* **2002**, *18*, 3694−3697.
(9) (a) Liz-Marzan, L. M.; Mulvaney, P. *J. Phys. Chem. B* **2003**, *107*, 7312−7326, (b) Collier, C. P.; Saykally, R. J.; Shiang, J. J.; Henrichs, S. E.; Heath, J. R. *Science* **1997**, *277*, 1978−1981.
(10) Liz-Marzan, L. M.; Giersig, M.; Mulvaney, P. *Langmuir* **1996**, *12*, 4329−4335.
(11) Ung, T.; Liz-Marzan, L. M.; Mulvaney, P. *J. Phys. Chem. B* **2001**, *105*, 3441−3452. For other results based on interparticle spacing see: (1) Schmitt, J.; Mächtle, P.; Eck, D.; Möhwald, H.; Helm. C. A. *Langmuir* **1999**, *15*, 3256−3266, (2) Hövel, H.; Fritz, S.; Hilger, A.; Kreibig, U. *Phys. Rev. B* **1993**, *48*, 18178−18188.
(12) Among the various effective medium theories available, it has been found that the Maxwell−Garnett theory is suitable to describe these dipole−dipole interactions; see: Maxwell−Garnett, J. C. *Philos. Trans. R. Soc. London*; **1904**, *203*, p 385.
(13) (a) West, J. L.; Halas, N. J. *Annu. Rev. Biomed. Eng.* **2003**, *5*, 285−292, (b) Storhoff, J. J.; Lazarides, A. A.; Mucic, R. C.; Mirkin, C. A.; Letsinger, R. L.; Schatz, G. C. *J. Am. Chem. Soc.* **2000**, *122*, 4640−4650.
(14) Frankamp, B. L.; Boal, A. K.; Rotello, V. M. *J. Am. Chem. Soc.* **2002**, *124*, 15146−15147.
(15) Teranishi, T.; Hasegawa, S.; Shimizu, T.; Miyake, M. *Adv. Mater.* **2001**, *13*, 1699−1701.
(16) Carroll, J. B.; Frankamp, B. L.; Srivastava, S.; Rotello, V. M. *J. Mater. Chem.* **2004**, *14*, 690−694.

10.1021/cm048579d CCC: $30.25
Published on Web 01/12/2005

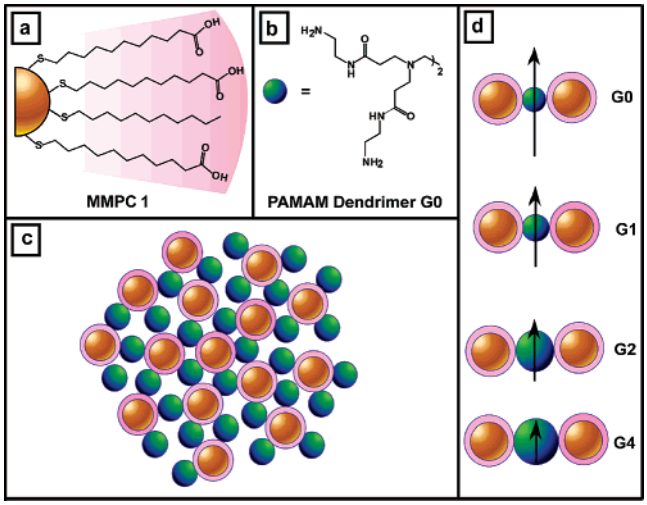

Figure 1. (a) MMPC **1** modified with carboxylic acids. (b) Structure for PAMAM G_0.(c) Self-assembly of MMPC **1** and PAMAM dendrimers. (d) Schematic of the relative decrease in dipolar coupling (arrow) upon assembly with various PAMAM generations.

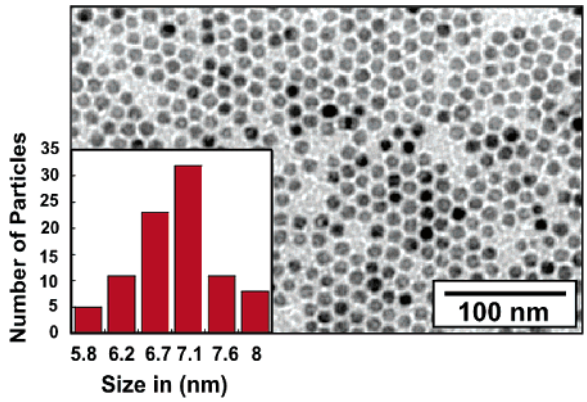

Figure 2. TEM analyses of MMPC **1** with the histogram (inset) showing an average particle diameter of 6.8 ± 0.7 nm.

nanoparticles. This precise structural control enabled us to systematically alter the collective SPR by mitigating the dipolar coupling between the nanoparticles. Small-angle X-ray scattering (SAXS) was used to quantify the increase in interparticle spacing followed by ultraviolet (UV) spectroscopy to track the change in SPR upon assembly. Finally, transmission electron microscopy (TEM) was employed to visualize the resulting aggregates.

Results and Discussion

The present study utilizes the "bricks and mortar" method, where a series of PAMAM dendrimers was used as "mortar" and monodisperse mixed monolayer protected clusters (MMPC **1**) (6.8 nm in size) were used as "bricks" (Figure 2). An electrostatic interaction between the terminal amine on the dendrimer and the carboxylic acid on MMPC **1** provided the driving force for self-assembly. To ensure that each nanoparticle was completely coated and consequently spaced by each generation of dendrimer, a solution of MMPC **1** was slowly added to an excess of the PAMAM dendrimer

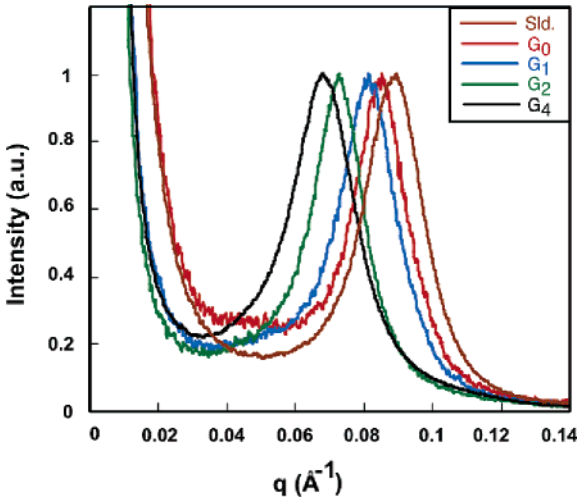

Figure 3. SAXS plot of MMPC **1** assembled with G_0−G_4 PAMAM dendrimer and the control (Sld).

Table 1. Spacing Values for PAMAM Dendrimers Assembled with MMPC 1

	solid[a]	G_0	G_0	G_2	G_4	solution[b]
q (Å^{-1})	0.089	0.085	0.081	0.073	0.068	
D (nm)[c]	7.15	7.39	7.80	8.62	9.20	
SPR(nm)	610	592	576	564	538	526

[a] MMPC **1** as solid film. [b] Gold nanoparticles (6.8 nm) in solution before place exchange. [c] Distances were calculated from the relation (distance) $D = 2\pi/Q$.

in MeOH. The mixture rapidly became turbid, followed by slow precipitation depending on the dendrimer generation; higher generations took longer time for complete precipitation (see below). The solution was allowed to fully precipitate, resulting in a thin film that was analyzed using SAXS and UV spectroscopy.

SAXS was used to quantify the interparticle spacing for MMPC **1** assembled with excess of PAMAM dendrimers G_0−G_4 (Figure 3). The q values, representative of average interparticle spacing, shifted steadily downward with increasing dendrimer generation (Table 1). The interparticle spacing values attained for each generation showed a regular trend of edge-to-edge spacing from 0.6 nm for G_0 to 1.9 nm for G_4. The observed surface-to-surface spacing of ∼1.9 nm for MMPC **1** assembled with G_4 indicates a constriction of the globular solution structure of the dendrimer (∼4.5 nm[18]) upon assembly, which is not surprising given the large free volume inherent in dendrimer molecules. The structure of dendrimer is not maintained during the assembly, because this structure constricts upon precipitation, especially for the lower generation dendrimers. Despite the constriction of the dendrimer upon assembly, the sequential increase in interparticle spacing was sufficient to dramatically alter the collective SPR[7,19] through modulation of dipolar coupling.

UV−Vis spectroscopy was used to analyze the SPR of each MMPC **1**/PAMAM sample, demonstrating the modulation of dipolar interactions upon assembly (Figure 4).[20] The

(17) (a) He, J. A.; Valluzzi, R.; Yang, K.; Dolukhanyan, T.; Sung, C. M.; Kumar, J.; Tripathy, S. K.; Samuelson, L.; Balogh, L.; Tomalia, D. A. *Chem. Mater.* **1999**, *11*, 3268−3274, (b) Sooklal, K.; Hanus, L. H.; Ploehn, H. J.; Murphy, C. J. *Adv. Mater.* **1998**, *10*, 1083−1087.

(18) Dendritech web site: Dendritech.com.

(19) Lazarides, A. A.; Schatz, G. C. *J. Chem. Phys.* **2000**, *112*, 2987−2993.

(20) To ensure sample consistency, the exact same MMPC **1**/PAMAM samples were used for SAXS and UV analysis.

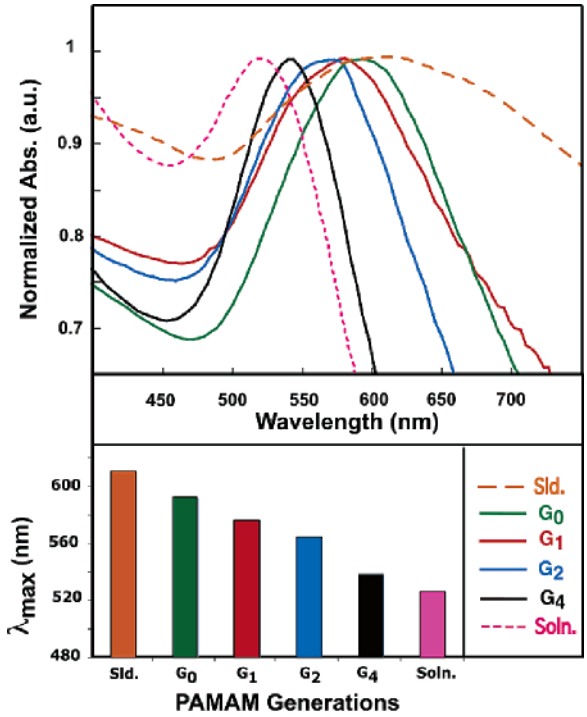

Figure 4. UV−visible studies on thin films of MMPC **1** assembled with G_0−G_4 dendrimers (G_0, G_1, G_2, and G_4), and the control spectra of MMPC **1** on solid surface (Sld) and free in solution (Soln).

SPR showed a steady blue shift as MMPC **1** was assembled with G_0 through G_4 (Table 1). To place these values in context, we compared the values obtained from the thin films to the maximal shift from solution SPR, assumed to be free of dipolar interactions following the analysis of Mulvaney.[12] We would predict a sequentially smaller shift from the free SPR as the interparticle spacing was increased. Indeed, G_4 showed nearly identical wavelength to that of the solution sample, while G_0 red shifted nearly 60 nm. The SPR values for G_0 through G_4 were also compared with that of the MMPC **1** thin film in the absence of dendrimers to present maximum dipolar interaction, demonstrating the ability to tune the resonance over an 84-nm range through directed self-assembly.

We observed a substantial difference in the length of time required for each system to fully precipitate. To quantify the different rates of precipitation and its effect on SPR shifts, we carried out a time course experiment (Figure 5).[21] In all the cases we saw a loss in intensity due to precipitation, with the largest dendrimer (G_4) requiring days to fully precipitate. This variation in rate arises from inherent differences between the interaction of small and large dendrimers with the particle surface. The assembly process begins by adding a solution of nanoparticles to an excess of dendrimer in MeOH solvent. It is reasonable to assume that in the initial solution each nanoparticle is coated completely in dendrimer, given the large excess of dendrimer. If this structure were static, then no precipitation would occur. Our system, however, is based on noncovalent interactions that allow for reorganization of the system to maximize the enthalpic interaction between

(21) Kinetic experiments were carried out at room temperature with slightly lower overall concentration, to allow for optical transparency, while the relative ratio of MMPC **1** and PAMAM dendrimer remained constant.

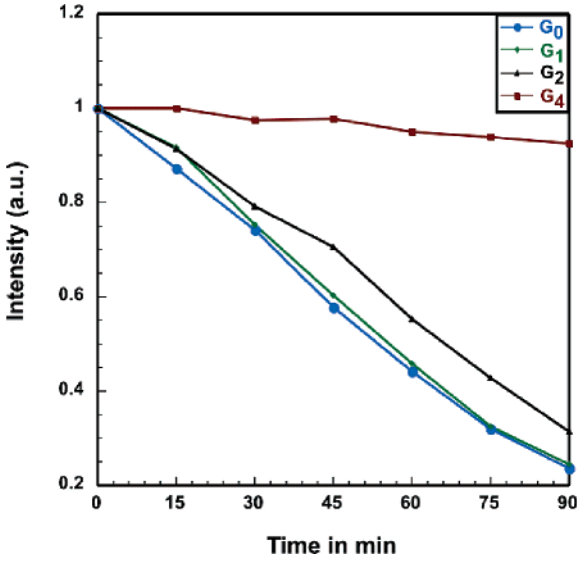

Figure 5. MMPC **1** assembled with G_0−G_4 shows a different rate of precipitation, as seen by a loss in SPR intensity at 520 nm.

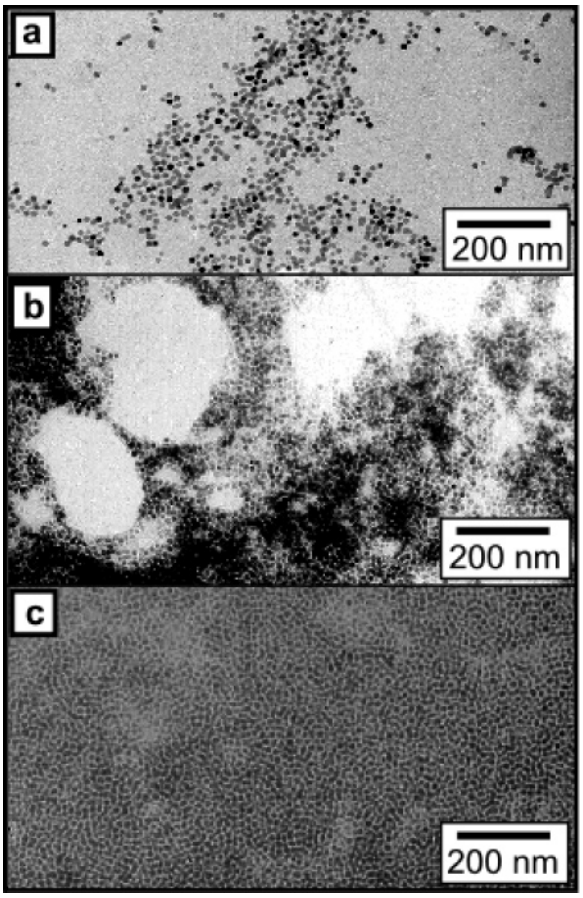

Figure 6. (a) Acid-functionalized MMPC **1** (NP1). (b) MMPC **1**−G_0 assembly upon precipitation. (c) MMPC **1**−G_4 assembly upon precipitation.

dendrimer and nanoparticle leading to cross-linking and ultimately precipitation. This reorganization occurs as the dendrimer equilibrates between bound and unbound states on the surface of MMPC **1**. The smaller dendrimers with fewer interactions would be expected to undergo a more rapid transition while the increased number of amine sites capable of multivalent electrostatic interaction on G_4 lead to a drastic reduction in the rate of this equilibrium as the cooperatively of the interaction slows the rate of dissociation.[22]

Finally, TEM was used to determine structural differences between unassembled particles and those assembled with PAMAM dendrimers. The TEM samples were prepared identically to the UV and SAXS samples; prepared through slow precipitation of a film of MMPC **1**−PAMAM on copper-coated TEM grids. MMPC **1** showed some self-association (Figure 6a) due to a combination of carboxylic acid dimerization and van der Waals contact. In contrast, MMPC **1**−G_0 composites showed a network-like structure indicative of rapid precipitation (Figure 6b).[23] MMPC **1**−G_4, on the other hand, resulted in more uniform film nanoparticles as a result of the slow precipitation process outlined above (Figure 6c).

In summary, we have shown that "bricks and mortar" self-assembly of optically active nanoparticles using PAMAM dendrimers leads to both structural and functional control of the resulting aggregates. The structural changes were quantified using SAXS, while the changes in SPR were monitored with UV spectroscopy. The ability to tune the SPR over a wide range of wavelengths using a stock solution of nanoparticles and commercially available dendrimers demonstrates the unique versatility of our system. Furthermore, it opens the door for the creation of pragmatic materials with tailored optical properties.

Experimental Section:

Materials. All poly(amidoamine) PAMAM starburst dendrimers G_0, G_1, G_2, and G_4; $HAuCl_4 \cdot 4H_2O$; $NaBH_4$; tetraoctylammonium bromide; and MeOH were purchased from Sigma-Aldrich.

Synthesis: Thermal Ripening Method. MMPC **1** was synthesized using our previously published procedure originally developed as stated in ref 15.

Characterization. *Small Angle X-ray Scattering (SAXS).* Samples for SAXS analysis were prepared by placing a ($\sim$1 cm^2) piece of Mylar film at the bottom of 2 mL vial to which MMPC **1** (0.5 mg/mL in MeOH) was added drop by drop to each dendrimer generation (0.5 mg/mL in MeOH) in (1:10) molar ratio. All samples were allowed to full precipitate. The remaining solution was then removed, and the samples were dried completely.

UV−Visible Spectroscopy (UV). UV studies were carried out with an 8452A HP diode array spectrophotometer. The SPR study was carried out in solution as well as on thin solid films. Thin films were prepared identical to SAXS samples and were analyzed under UV. For the solution study, a kinetic run was carried out for 90 min. For sample preparation, 0.1 mL of MMPC **1** (0.05 mg/mL in MeOH) was added drop-by-drop to 0.9 mL of dendrimer solution and then sampled over time with each PAMAM generation (G_0, G_1, G_2 and G_4) in solution.

Transmission Electron Microscopy (TEM). The samples were prepared by placing the TEM grid inside the 2 mL vial, and the aggregate was precipitated on the 300 Cu mesh/carbon film TEM sample grids. Samples were then analyzed using a JEOL 200CX electron microscope with an acceleration voltage of 200 keV.

Acknowledgment. This research was supported by the National Science Foundation (NSF; CHE-0213354, MRSEC facilities, and CHE CHE-0304173). B.L.F. acknowledges the 2003 American Chemical Society Organic Division graduate fellowship, sponsored by Procter and Gamble, and the University of Massachusetts, Amherst graduate student fellowship for 2004.

Supporting Information Available: Solution UV−vis study of SPR and atomic force micrographs of nanocomposites (pdf). This material is available free of charge via the Internet at http://pubs.acs.org.

CM048579D

(22) PAMAM generation 6 never precipitated, even though the molar ratios of nanoparticle to dendrimer are identical in all cases.

(23) Boal, A. K.; Galow, T. H.; Ilhan, F.; Rotello, V. M. *Adv. Funct. Mater.* **2001**, *11*, 461−465.